Supporting information

V(III) Doped Nickel Oxide-Based Nanocatalysts for Electrochemical Water Splitting: Influence of Phase, Composition, and Doping on the Electrocatalytic Activity

Daniel Böhm[1,2], Michael Beetz[1], Christopher Kutz[1], Siyuan Zhang[4], Christina Scheu[4,5], Thomas Bein[1*] and Dina Fattakhova-Rohlfing[2,3*]

[1]Department of Chemistry and Center for NanoScience (CeNS), Ludwig-Maximilians-Universität München (LMU Munich), Butenandtstrasse 5-13 (E), 81377 Munich, Germany

[2]Institute of Energy and Climate Research (IEK-1) Materials Synthesis and Processing, Forschungszentrum Jülich GmbH, Wilhelm-Johnen-Strasse, 52425 Jülich, Germany

[3]Faculty of Engineering and Center for Nanointegration Duisburg-Essen (CENIDE), University of Duisburg-Essen, Lothar-straße 1, 47057 Duisburg, Germany

[4]Max-Planck-Institut für Eisenforschung (MPIE) GmbH & RWTH Aachen, Max-Planck-Straße 1, 40237 Düsseldorf

[5]Materials Analytics, RWTH Aachen University, Kopernikusstrasse 10, 52074 Aachen, Germany

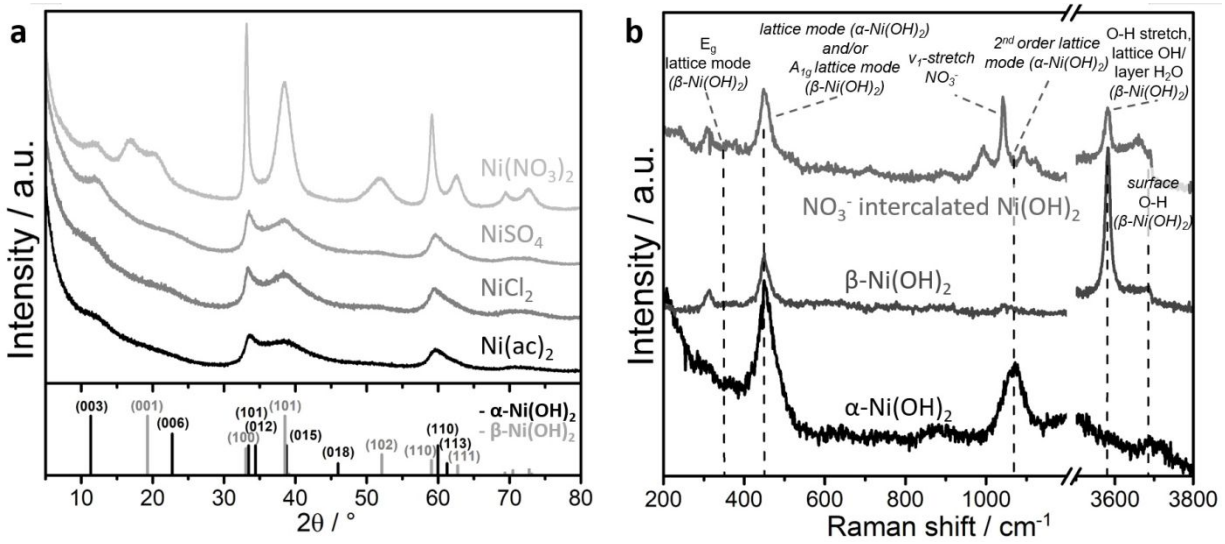

Figure S1 X-ray diffractogramms (a) of nanocatalyst prepared by rapid precipitation method with different Ni(II)-precursors and Raman spectra (b) of nitrate anion intercalated $Ni(OH)_2$. α-$Ni(OH)_2$ ($Ni(OH)_2$ x 0.75 H_2O) pattern: ICDD card number 00-038-0715 (rhombohedral, a = b = 3.08 Å, c = 23.41 Å, α = β = 90°, γ = 120°). β-$Ni(OH)_2$ ($Ni(OH)_2$) pattern: ICDD card number 00-014-0117 (hexagonal, a = b = 3.126, c = 4.605, α = β = 90°, γ = 120°). The bands at 450 cm^{-1} (lattice mode) and 1070 cm^{-1} (2nd order lattice mode) were assigned to the α-$Ni(OH)_2$ phase.[1-2] Bands at 447 cm^{-1} (A_{1g} lattice mode), 3581 cm^{-1} (O-H stretch / lattice OH / layer H_2O mode) and 3690 cm^{-1} (surface O-H stretch) were assigned to the β-$Ni(OH)_2$ phase.[2]

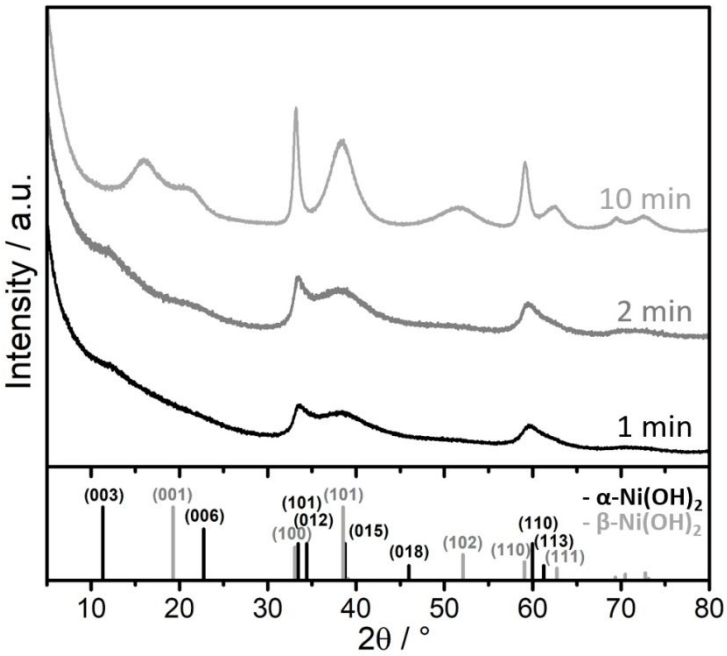

Figure S2 X-ray diffractograms of $Ni(OH)_2$ products obtained by the rapid precipitation method with KO_2 with variation of reaction time before quenching. Synthesis performed at room temperature. α-$Ni(OH)_2$ ($Ni(OH)_2$ x 0.75 H_2O) pattern: ICDD card number 00-038-0715 (rhombohedral, a = b = 3.08 Å, c = 23.41 Å, α = β = 90°, γ = 120°). β-$Ni(OH)_2$ ($Ni(OH)_2$) pattern: ICDD card number 00-014-0117 (hexagonal, a = b = 3.126 Å, c = 4.605 Å, α = β = 90°, γ = 120°).

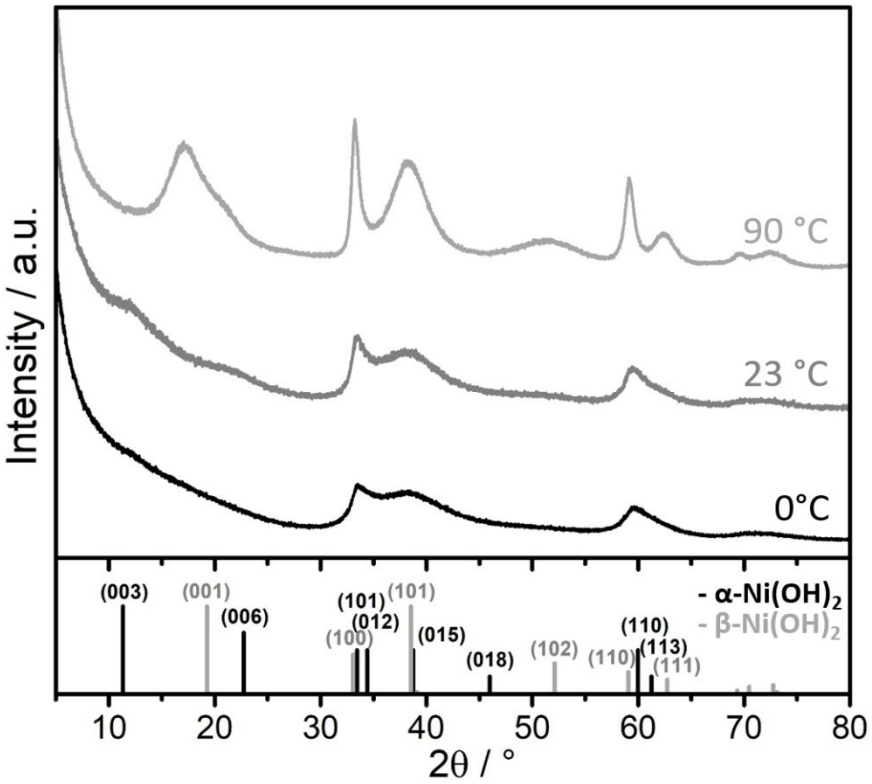

Figure S3 X-ray diffractograms of $Ni(OH)_2$ products obtained by rapid precipitation method with KO_2 with variation of synthesis temperature. Synthesis performed with 2 min reaction time before quenching. α-$Ni(OH)_2$ ($Ni(OH)_2$ x 0.75 H_2O) pattern: ICDD card number 00-038-0715 (rhombohedral, a = b = 3.08 Å, c = 23.41 Å, α = β = 90°, γ = 120°). β-$Ni(OH)_2$ ($Ni(OH)_2$) pattern: ICDD card number 00-014-0117 (hexagonal, a = b = 3.126 Å, c = 4.605 Å, α = β = 90°, γ = 120°).

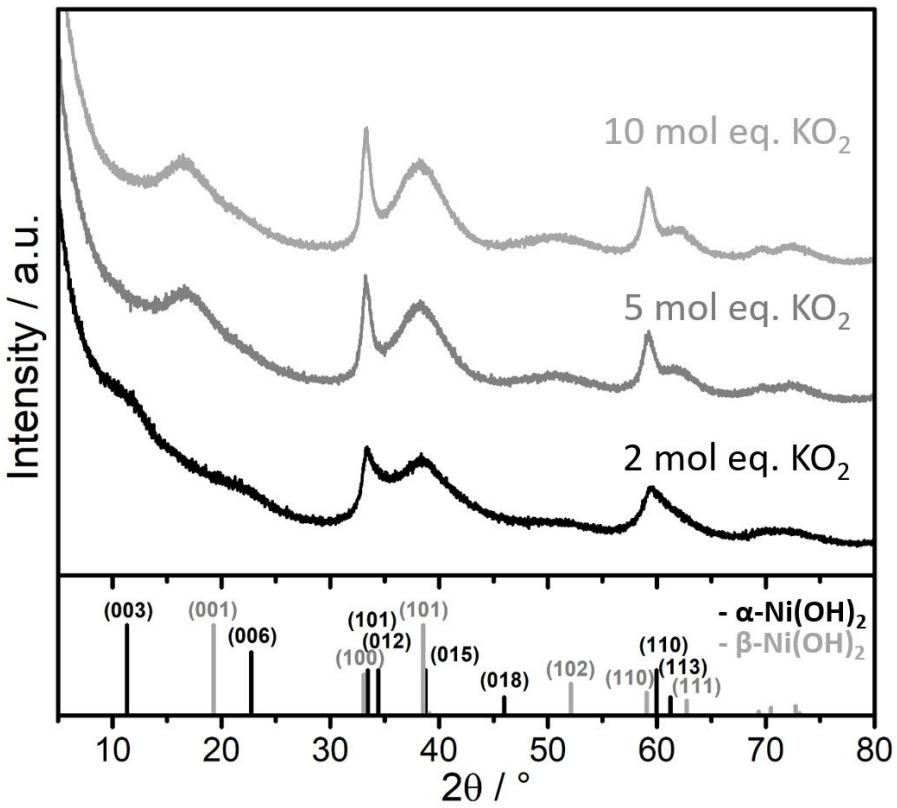

Figure S4 X-ray diffractograms of $Ni(OH)_2$ products obtained by rapid precipitation method with varied amounts of KO_2. Synthesis was performed with 2 min reaction time before quenching each at 0 °C. α-$Ni(OH)_2$ ($Ni(OH)_2$ x 0.75 H_2O) pattern: ICDD card number 00-038-0715 (rhombohedral, a = b = 3.08 Å, c = 23.41 Å, α = β = 90°, γ = 120°). β-$Ni(OH)_2$ ($Ni(OH)_2$) pattern: ICDD card number 00-014-0117 (hexagonal, a = b = 3.126 Å, c = 4.605 Å, α = β = 90°, γ = 120°).

Table S 1 Elemental analysis via inductively coupled plasma optical emission spectrometry (ICP-OES) of V(III)-doped $Ni_{1-x}V_x(OH)_2$ Cl^-

doping element	precursor	doping level / at%	ICP-OES / at%
pure $Ni(OH)_2$	$NiCl_2$	0	N/A
V(III)	$NiCl_2$ + VCl_3	1	1.0
V(III)	$NiCl_2$ + VCl_3	2	2.1
V(III)	$NiCl_2$ + VCl_3	5	4.9
V(III)	$NiCl_2$ + VCl_3	10	9.7
V(III)	$NiCl_2$ + VCl_3	15	15.4
V(III)	$NiCl_2$ + VCl_3	50	38.6
pure vanadium compound	VCl_3	100	N/A

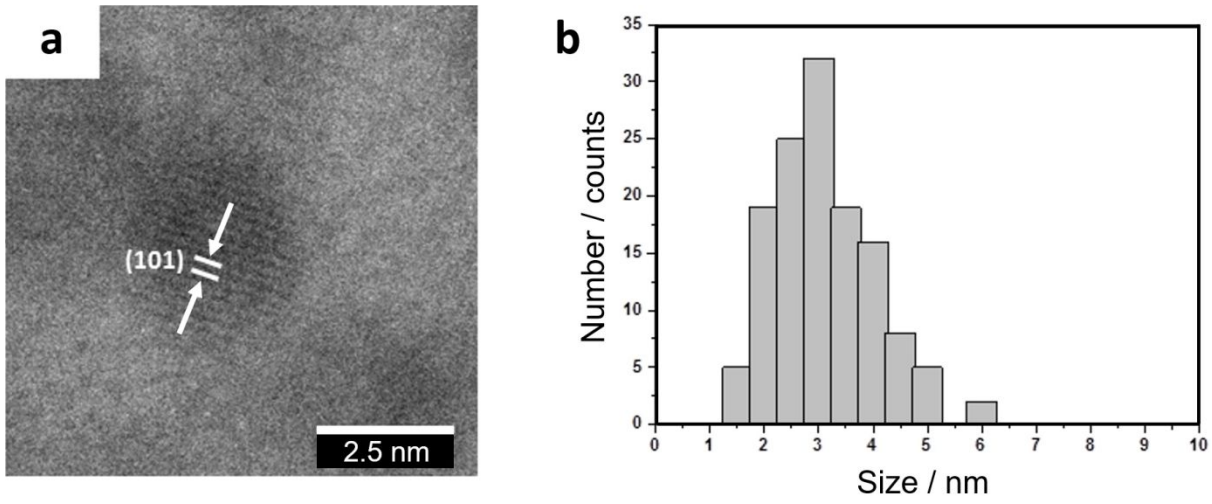

Figure S5 (a) Transmission electron micrograph of single β-Ni(OH)$_2$ nanoparticle. (b) Size distribution determined from particles imaged by TEM. Indexing of d-spacings of β-Ni(OH)$_2$ nanoparticle according to β-Ni(OH)$_2$ pattern: ICDD card number 00-014-0117 (hexagonal, a = b = 3.126 Å, c = 4.605 Å, α = β = 90°, γ = 120°).

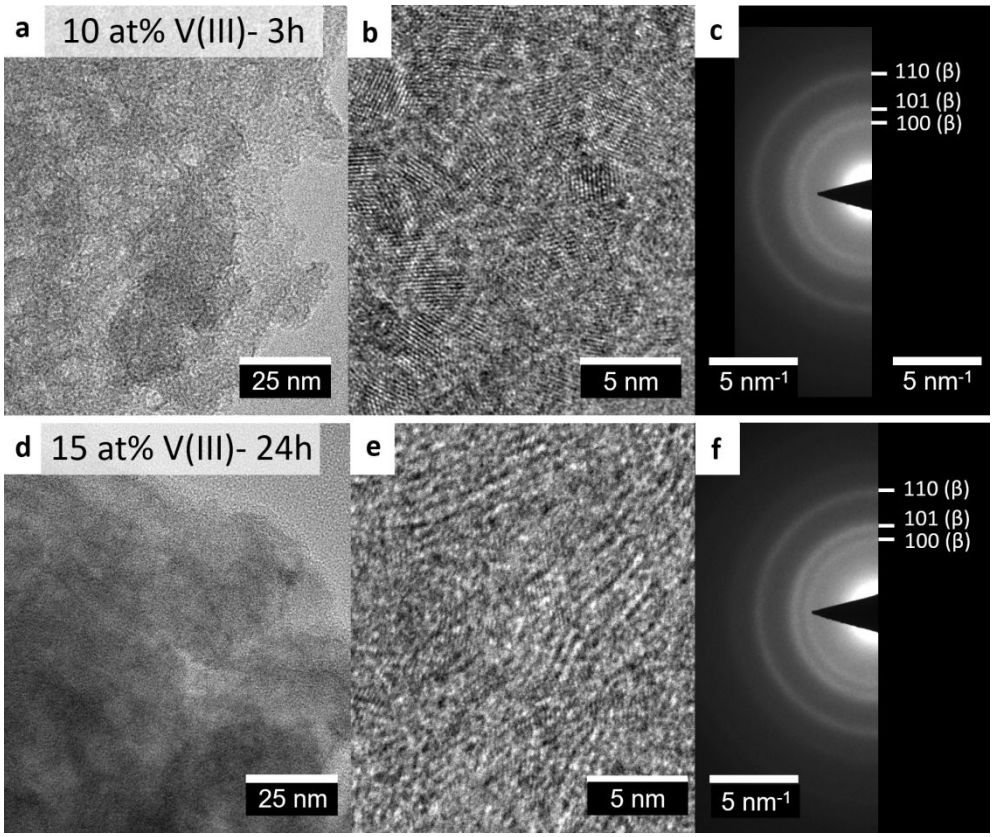

Figure S6 Structural characterization of time-dependent phase transformations of V(III) doped Ni(OH)$_2$ by transmission electron microscopy. TEM images and electron diffraction pattern of 10 at% V(III) doped Ni(OH)$_2$ after 3 h (a-c) and 15 at% V(III) doped Ni(OH)$_2$ after 24 h (d-f) aging time. β-Ni(OH)$_2$ (Ni(OH)$_2$) pattern: ICDD card number 00-014-0117 (hexagonal, a = b = 3.126 Å, c = 4.605 Å, α = β = 90°, γ = 120)

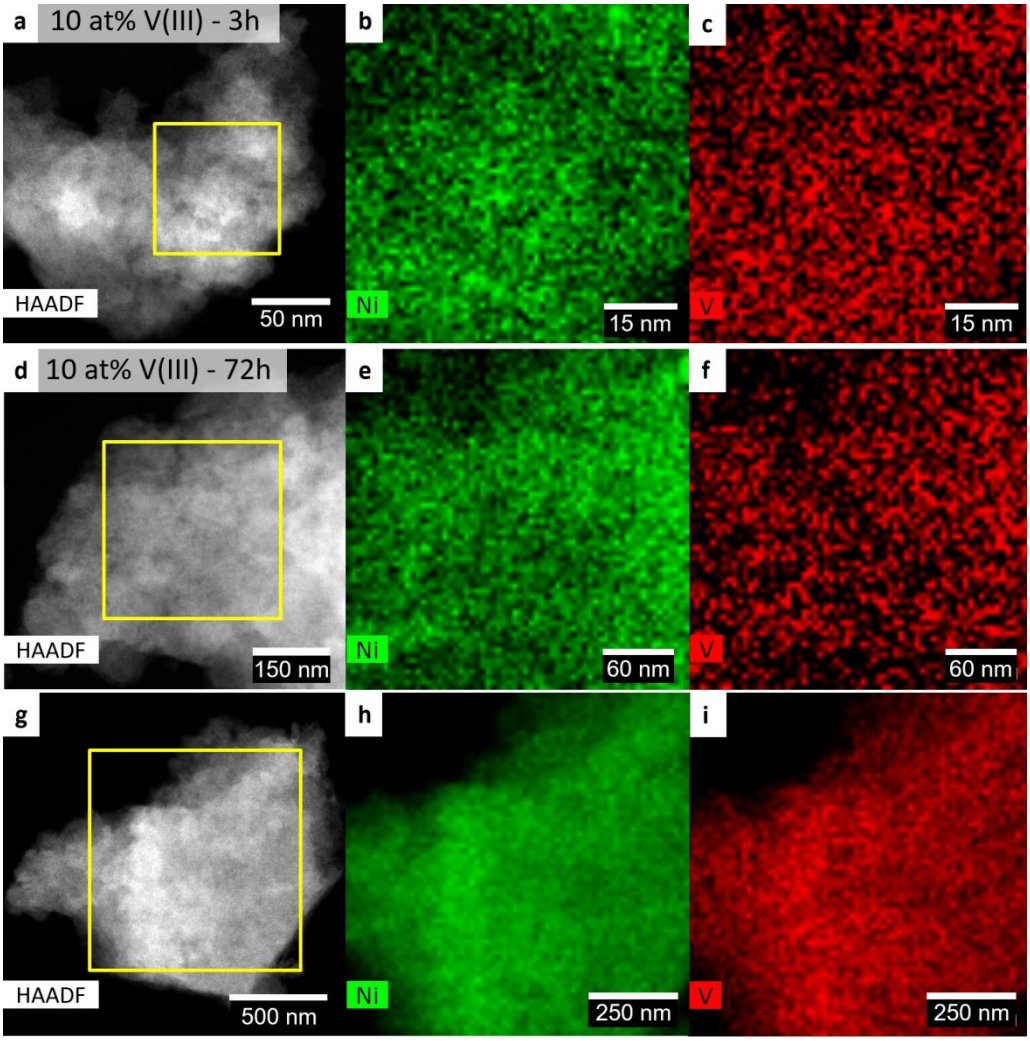

Figure S7 STEM-EDX and energy-dispersive X-ray spectroscopy mapping of V(III) doped $Ni(OH)_2$ at different length scales. STEM-EDX mappings of 3 h aged 10 at% V(III) doped sample (a-c). STEM-EDX mappings of 72 h aged 10 at% V(III) doped, at medium (d-f) and lower (g-i) magnification.

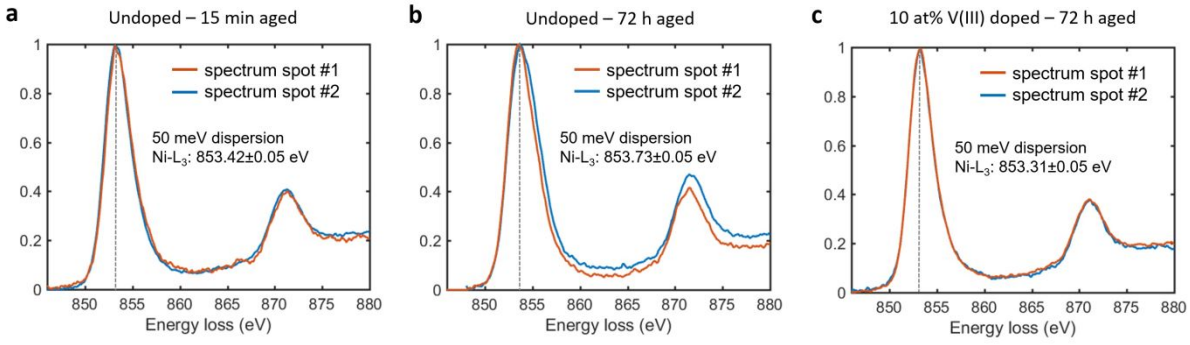

Figure S8 Characterization of the electronic structure of nickel in aged and V(III)-doped samples by electron energy loss spectroscopy. EELS spectra with 50 meV dispersion of (a) undoped 15 min, (b) undoped 72 h and (c) 10 at% V(III) 72 h aged $Ni(OH)_2$ samples.

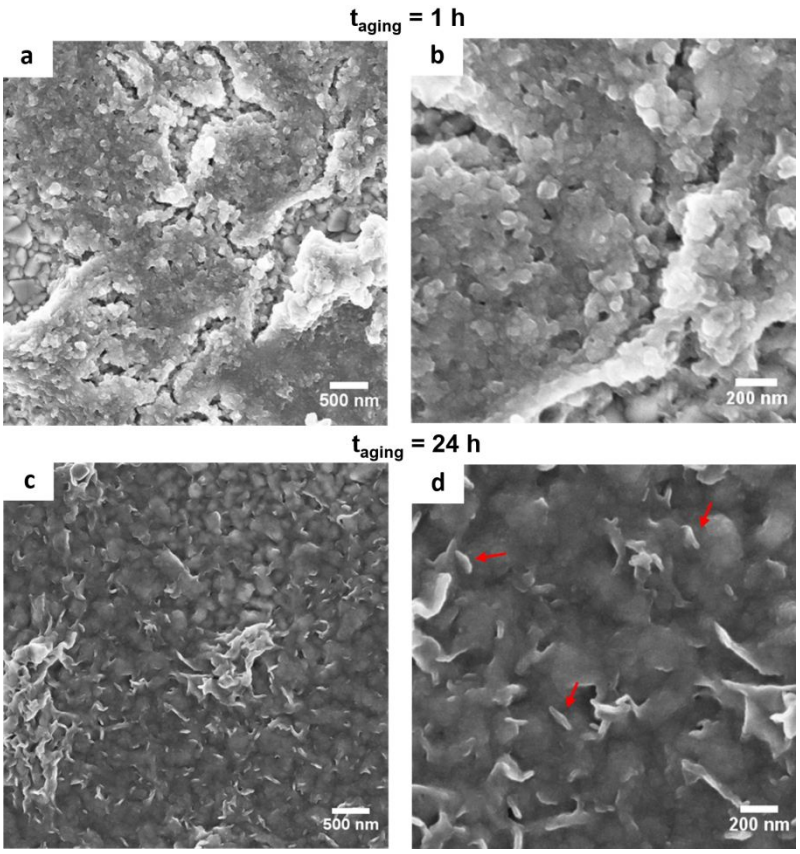

Figure S9 Scanning electron micrographs of $Ni(OH)_2$ based electrodes for electrochemical characterization. (a-d) Top-view of 1 h (a, b) and 24 h (c, d) aged undoped $Ni(OH)_2$ dropcasted on an FTO substrate with loadings of ~50 µg cm^{-2}.

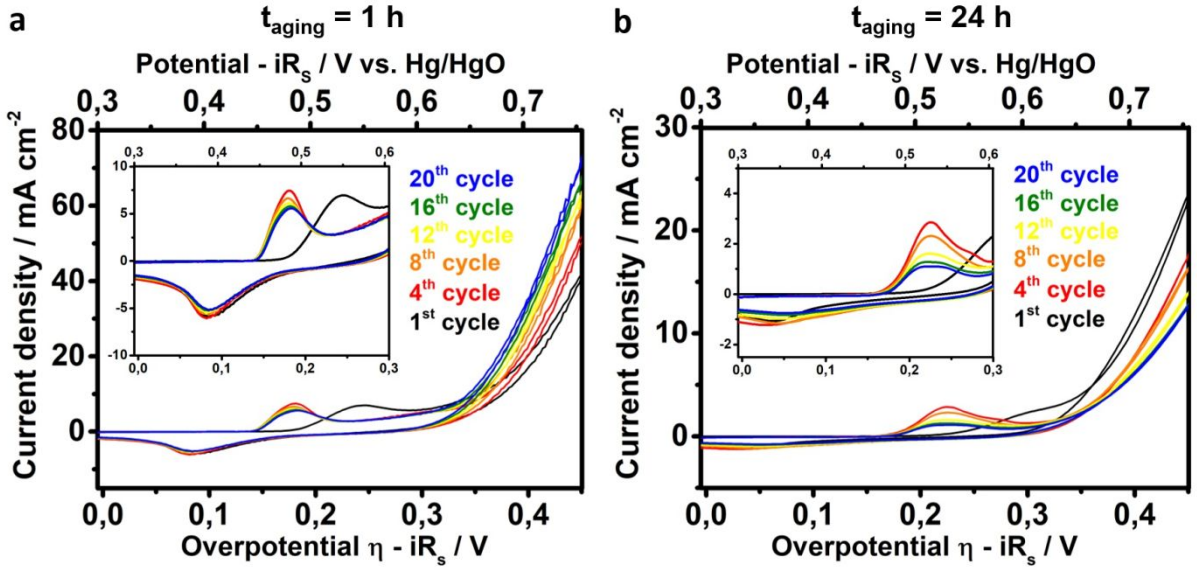

Figure S10 Electrochemical characterization of chemically aged $Ni(OH)_2$. Cyclic voltammograms (1st, 4th, 8th, 12th, 16th and 20th scan cycle) of 1 h (a) and 24 h (b) aged undoped $Ni(OH)_2$.

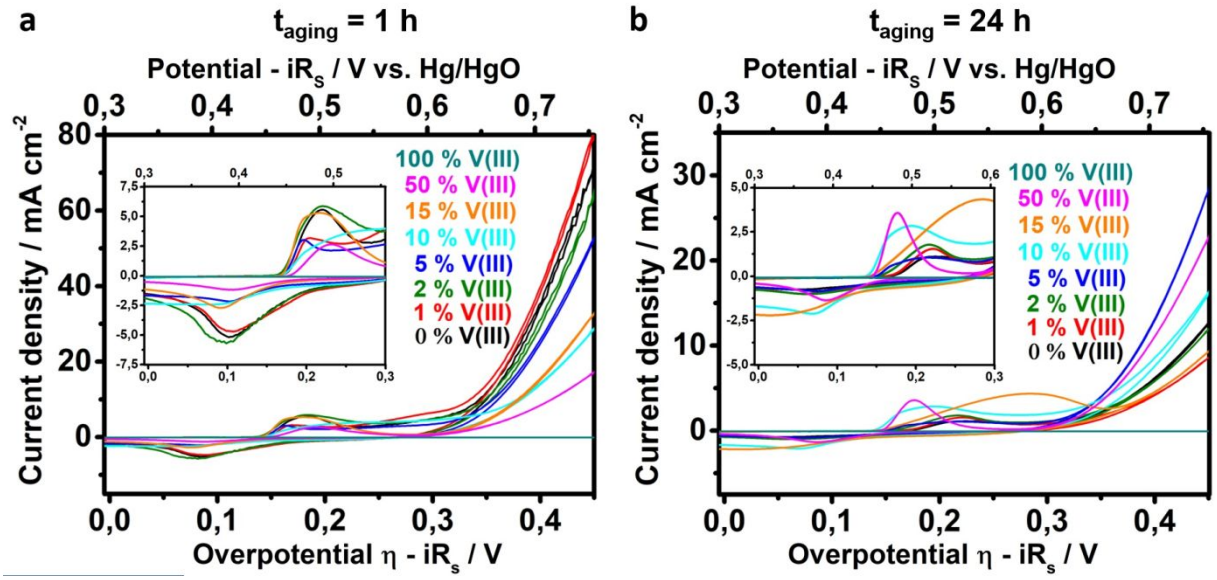

Figure S11 Electrochemical characterization of chemically aged and V(III) doped $Ni(OH)_2$. Cyclic voltammograms (20th scan cycle) of 1 h (a) and 24 h (b) aged 0, 1, 2, 5, 10, 15, 50 and 100 at% V(III) containing $Ni(OH)_2$.

Table S2 Results obtained from the electrochemical characterization of 1 h chemically aged $Ni_{1-x}V_x(OH)_2$ obtained in the 20th cycle

V(III) content / at%	mass loading (determined) / µg cm^{-2}	E_a / η in mV	E_c / η in mV	Redox potential E_{red} / η in mV	η at 10 mA cm^{-2} / mV	current density j at η = 350 mV / mA cm^{-2}	current density j at η = 400 mV / mA cm^{-2}
0	N/A[a]	184	84	134	344	10.91	34.48
1	N/A[a]	169	88	128.5	335	12.64	38.05
2	N/A[a]	184	82	133	350	9.59	29.53
5	N/A[a]	163	84	123.5	357	7.90	24.74
10	60.8	N/A[b]	N/A[b]	N/A[b]	379	5.59	13.81
15	70.7	177	77	127	379	4.44	14.98
50	35.6	N/A[b]	N/A[b]	N/A[b]	411	2.95	8.24
100	24.7	N/A[b]	N/A[b]	N/A[b]	> 900	0.01	0.01

[a] No mass loading could be determined. [b] No value listed due to a broad and undefined peak.

Table S3 Results obtained from the electrochemical characterization of 24 h chemically aged $Ni_{1-x}V_x(OH)_2$ obtained in the 20th cycle

V(III) content / at%	mass loading (determined) / µg cm^{-2}	E_a / η in mV	E_c / η in mV	Redox potential E_{red} / η in mV	η at 10 mA cm^{-2} / mV	current density j at η = 350 mV / mA cm^{-2}	current density j at η = 400 mV / mA cm^{-2}
0	72.7	221	49	135	433	2.48	6.78
1	72.7	220	54	137	459	1.77	4.64
2	71.7	216	62	139	438	2.46	6.45
5	66.8	218	77	148	389	4.59	14.64
10	N/Aa	191	68	130	411	3.39	8.91
15	85.9	284	15	150	458	2.23	5.01
50	21.7	176	86	131	396	3.96	12.31
100	19.7	N/A[b]	N/A[b]	N/A[b]	> 900	0.01	0.01

[a] No mass loading could be determined. [b] No value listed due to a broad and undefined peak.

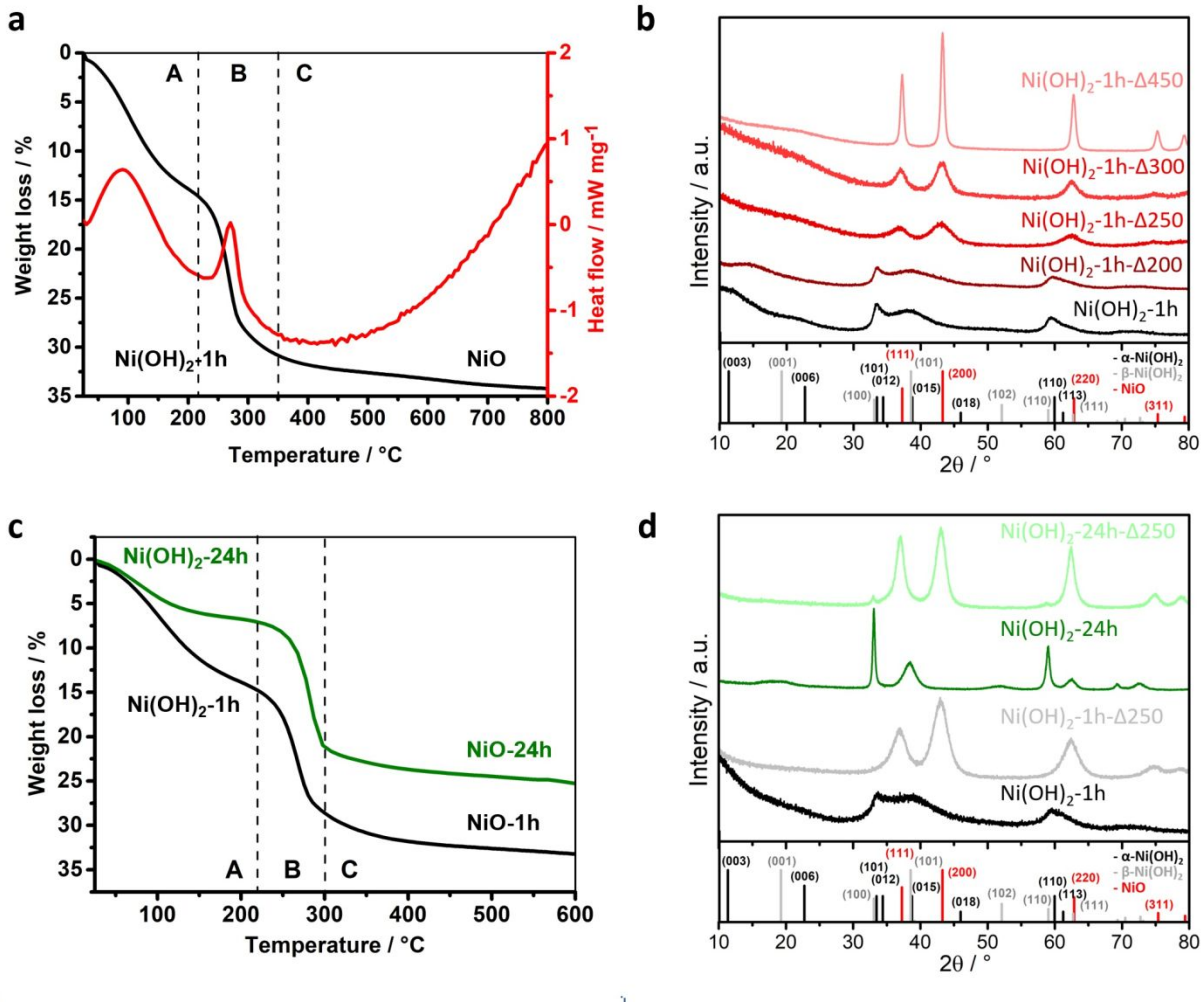

Figure S12 Structural characterization of aged $Ni(OH)_2$ upon calcination. (a) Thermogravimetric analysis (black curve) and differential scannning calorimetry (red curve) of 1 h aged $Ni(OH)_2$ sample. (b) X-ray diffractogram of 200 – 450°C (red curves) calcined 1 h aged $Ni(OH)_2$ sample. (c) TGA of 1 h (black curve) and 24 h (green curve) aged $Ni(OH)_2$ samples. (d) XRD of calcined 1 h aged (black and grey curve) and 24 h aged (dark and light green curve) $Ni(OH)_2$. α-$Ni(OH)_2$ ($Ni(OH)_2$ x 0.75 H_2O) pattern: ICDD card number 00-038-0715 (rhombohedral, a = b = 3.08 Å, c = 23.41 Å, α = β = 90°, γ = 120°). β-$Ni(OH)_2$ ($Ni(OH)_2$) pattern: ICDD card number 00-014-0117 (hexagonal, a = b = 3.126 Å, c = 4.605 Å, α = β = 90°, γ = 120°). NiO pattern: ICDD card number 01-071-1179 (cubic, a = b = c = 4.178 Å, α = β = γ = 90°)

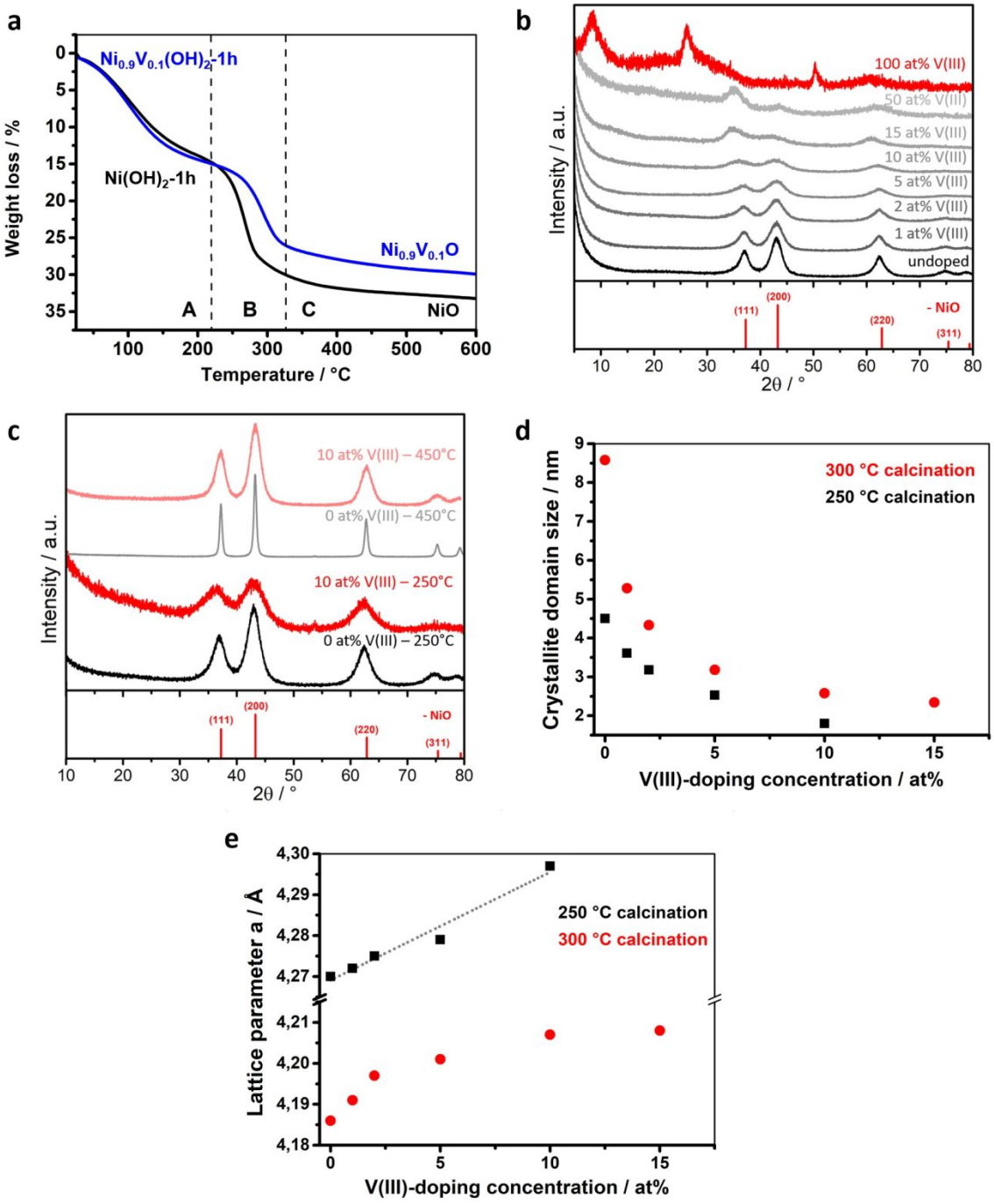

Figure S13 Structural characterization of calcined $Ni_{1-x}V_x(OH)_2$. (a) Thermogravimetric analysis of 1 h chemically aged undoped and 10 at% V(III) containing $Ni(OH)_2$. (b) X-ray diffractograms of V(III) doped (0-100 at% V(III) - greyscale and red curves) $Ni(OH)_2$ calcined at 250 °C. (c) XRD of undoped and $Ni_{0.9}V_{0.1}(OH)_2$ calcined at 250 °C (black, red curve) and 450 °C (grey, light red curve). NiO pattern: ICDD card number 01-071-1179 (cubic, a = b = c = 4.178 Å, α = β = γ = 90°) (d) Crystallite domain sizes of 250 °C (black) and 300 °C (red) calcined $Ni_{1-x}V_x(OH)_2$ derived from XRD line broadening according to Scherrer's equation. Graphical representation of data listed in Table S4 and S5. (e) Lattice parameter a of 250 °C (black) and 300 °C (red) calcined $Ni_{1-x}V_x(OH)_2$ calculated from the position (Gaussian fitted center of broadened reflection) of the NiO phase (200) reflection. Linear regression for 0-10 at% V(III) (dashed grey line) added for 250 °C calcined sample series. Graphical representation of data listed in Table S4 and S5.

Table S4: Calculated particle/domain sizes and lattice parameter *a* (NiO phase) based on the broadening of the 200 reflection in $Ni_{1-x}V_xO$ after calcination at 250 °C according to the Scherrer equation

V(III) content / at%	particle size / nm	Position /° 2Θ	lattice parameter *a* / Å
0	8.6	43.197	4.186
1	5.3	43.147	4.191
2	4.3	43.098	4.197
5	3.2	43.056	4.201
10	2.6	42.995	4.207
15	2.3	42.993	4.208

Table S5: Calculated particle/domain sizes and lattice parameter *a* (NiO phase) based on the broadening of the 200 reflection in $Ni_{1-x}V_xO$ after calcination at 300 °C according to the Scherrer equation

V(III) content / at%	particle size / nm	position /° 2Θ	lattice parameter *a* / Å
0	4.5	43.010	4.270
1	3.6	42.961	4.272
2	3.2	42.913	4.275
5	2.5	42.834	4.279
10	1.8	42.504	4.297

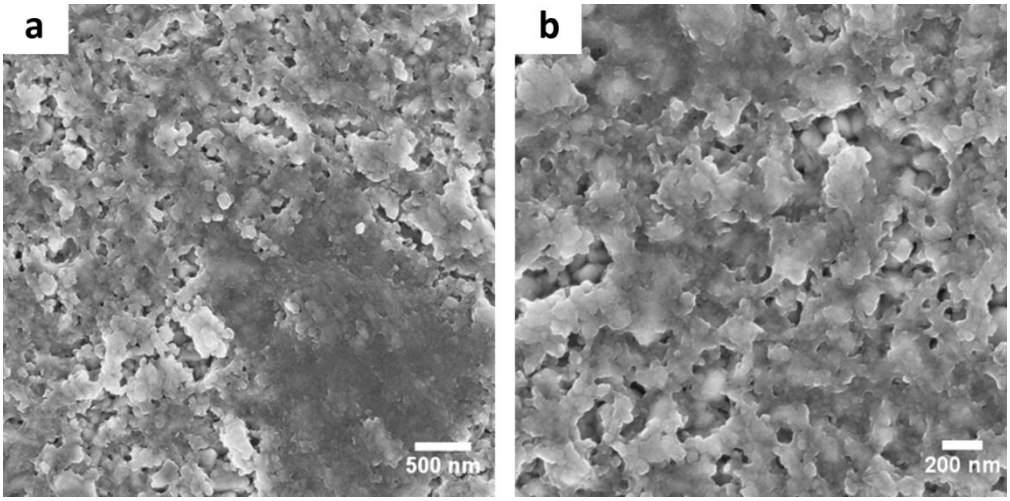

Figure S14 Scanning electron micrographs of NiO-based electrodes for electrochemical characterization. (a, b) Top-view of 1 h aged undoped $Ni(OH)_2$ dropcasted on an FTO substrate and calcined at 250 °C with loadings of ~50 µg cm^{-2}.

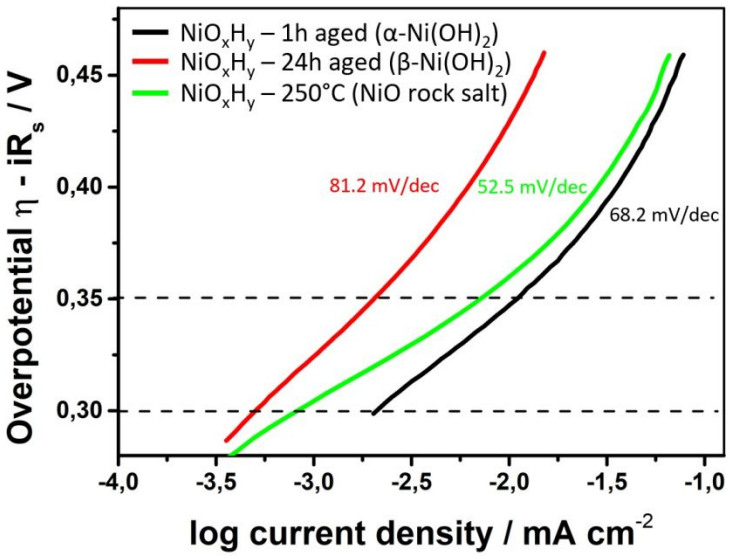

Figure S15 Tafel plot of chemically aged and calcined nickel hydroxide phases. Tafel plot of NiO_xH_y 1 h aged (black), 24 h aged (red) and 250 °C calcined (green) product.

REFERENCES

1. Hall, D. S.; Lockwood, D. J.; Poirier, S.; Bock, C.; MacDougall, B. R., Raman and Infrared Spectroscopy of α and β Phases of Thin Nickel Hydroxide Films Electrochemically Formed on Nickel. *J. Phys. Chem. A* **2012,** *116* (25), 6771-6784.
2. Hall, D. S.; Lockwood, D. J.; Poirier, S.; Bock, C.; MacDougall, B. R., Applications of in Situ Raman Spectroscopy for Identifying Nickel Hydroxide Materials and Surface Layers during Chemical Aging. *ACS Appl. Mater. Inter.* **2014,** *6* (5), 3141-3149.